Measurement of the self-broadening of the H_2 $Q(0-5)$ Raman transitions from 295 to 1000 K

Larry A. Rahn and R. L. Farrow
Combustion Research Facility, Sandia National Laboratories, Livermore, California 94551-0969

G. J. Rosasco
Center for Chemical Technology, National Institute of Standards and Technology, Gaithersburg, Maryland 20899
(Received 26 November 1990)

High-resolution inverse Raman spectroscopy has been used to measure the self-broadening coefficients of the Raman Q-branch transitions in pure (natural) hydrogen. Measurements of six lines [$Q(0)$–$Q(5)$] were made at pressures from 2 to 50 atm and from 295 to 1000 K. The dependence of the derived broadening coefficients on temperature and rotational quantum number is analyzed using the energy-corrected sudden scaling law [A. E. DePristo, J. Chem. Phys. **73**, 2145 (1980)]. We discuss three models for the J dependence of the pure-vibrational dephasing and find that models with little or no J dependence in the pure-vibrational dephasing are preferred.

I. INTRODUCTION

The study of collisional broadening of gas-phase spectra holds considerable promise for the furthering of our understanding of intermolecular interactions and collisional processes. This understanding is important in many endeavors. In the diagnosis of combustion processes, the application of spectroscopic techniques as measurement tools requires a predictive capability for spectra acquired under a very broad range of conditions. While extensive parametrization of collisional broadening and shift coefficients allows simple spectral models to be constructed, more complex phenomena such as Dicke narrowing,[1] collisional collapse,[2] and collisional speed-dependent effects[3] require deeper insights into the nature of collisional processes. Molecular hydrogen has long been of interest in fundamental studies of collisional processes because of its calculational simplicity and because its rovibrational spectra are easily obtained by a number of techniques. We have extended these studies to higher temperatures to study collisional processes characteristic of combustion environments.

The first systematic measurements of H_2 Raman Q-branch density broadening and shift by May *et al.*[4,5] were motivated by an interest in understanding the forces between nonpolar molecules. It was expected that the broadening and shift of the isotropic Raman Q branch with density would be a measure of vibrational rather than rotational perturbations as is the case for anisotropic scattering. Van Kranendonk[6] argued, however, using Anderson-theory[7] calculations of collisional broadening rates, that rotationally inelastic collisions are responsible for H_2 Q-branch density broadening. Allin *et al.*[8] noted that Van Kranendonk's calculations agreed with their measurement of the room-temperature self-broadening of the $Q(0)$ and $Q(2-3)$ lines in H_2 but that the observed $Q(1)$ broadening was more than twice that calculated. These authors concluded that the extra $Q(1)$ width is due to elastic vibrational dephasing, possibly associated with the "coupling shift" proposed by May *et al.*[5] for density shifts. Hunt, Barnes, and Brannon[9] repeated the calculation using different molecular constants, but the results reflected the same $Q(1)$ discrepancy. Kelley and Bragg[10] calculated the broadening due to elastic vibrational dephasing for temperatures of 50–500 K; the resulting $Q(1)$ elastic contribution at 300 K roughly accounted for the disagreement between experimental collision widths and Van Kranendonk's purely inelastic result. That elastic dephasing proves to be the major source of broadening for $Q(1)$ underscores the importance of this process for H_2 line broadening. Although the coupling shift was included in the interaction potential used by Kelley and Bragg, an associated J-dependent elastic broadening was not discussed in their report. The relative importance of rotational inelasticity and elastic vibrational dephasing in the H_2 Raman Q-branch linewidths has often been discussed in the literature[4–6,8–15] and is one of the particularly interesting aspects of collisional broadening in this system.

Our interest in identifying contributions to the collisional line shape is motivated by a desire to understand how different collisional processes contribute to the observed spectra under diverse conditions. The rotationally inelastic and elastic vibrational dephasing contributions to Q-branch linewidths, for example, arise from different terms in the interaction potential and their relative importance can vary greatly with the internal quantum state and with the collisional environment. An advantage of the H_2-H_2 system for distinguishing collisional processes is that the collisional perturbations are weak (the lines are narrow compared to the hard-sphere collision rate), allowing us to consider the contributions of various line-broadening processes as independent and additive.[10] While detailed scattering calculations are the most critical test of our knowledge of collisional processes, rigorous calculational methods are still being developed[16] and are difficult and expensive to implement. The analysis of J- and T-dependent broadening coefficients using scaling or rate laws to model the contributions of collisional processes has proved useful in many

cases.[14,15,17–21] Two studies in particular that are closely related to the present study analyzed the vibrational dephasing contributions to D_2 self- and foreign-gas-broadening[14] and to HD self-broadening[15] using an exponential energy-gap rate law to model rotationally inelastic rates.

When several collisional processes are important, comprehensive measurements are needed to gain insight from the application of rate law models. In the case of pure H_2, much work has been accomplished toward this end. The temperature dependence of the Q-branch broadening and shift coefficients from 80 to 315 K have been established from numerous measurements[4,5,8–13,22–30] with a few measurments[11,13] on $Q(1)$ to near 500 K in pure H_2. Density-shift and broadening data from quadrupole and induced-dipole absorption spectroscopy have been compared recently to Raman data and scattering theory by Kelley and Bragg.[10] Measurements have also been reported for the anisotropic (depolarized) H_2 Q-branch[30] and for pure rotational Raman spectra.[31] We have also recently reported[32] density-shift coefficients for the first six $[Q(0-5)]$ Q-branch transitions of H_2 between 295 and 1000 K.

In this paper, we report the self-broadening coefficients of the H_2 Raman Q-branch transitions ($J=0-5$) at temperatures between 295 and 1000 K. We fit the J and T dependence of these coefficients using the energy-corrected sudden (ECS) scaling law developed by DePristo.[33] Contributions from resonant rotation-rotation (R-R), rotation-translation (R-T), and elastic vibrational dephasing processes are included to account for the collisional line broadening. Strong R-R contributions and elastic vibrational dephasing processes are required to account for the T and J dependence of the self-broadening coefficients. We also investigate three different assumptions for the J and T dependence of the elastic vibrational dephasing contribution by fitting to our data and then comparing the predicted rotationally inelastic rates with published direct measurements as well as those derived from pure-rotational Raman linewidths.

II. EXPERIMENT

The IRS spectrometer and related experimental apparatus used in this study has been described previously[32] and will be discussed only briefly here. Raman spectra are acquired with a spectral resolution of ~ 0.0015 cm^{-1} using a pulse-amplified ($\sim$22-ns pulse width) cw dye laser as a pump and a single-frequency argon-ion laser as a probe. The probe-laser frequency is locked to a temperature-stabilized (750-MHz free spectral range) etalon, which also provides pump-laser-transmission fringes that are used to linearize the pump-laser scan. An accuracy of ± 0.0005 cm^{-1} for each data point relative to the start of the scan is achieved. The IRS signal is linear in the power density of the pump and probe lasers. We have found that the measured IRS signal voltage is very linear in the measured pump energy when the lasers are carefully cofocused and the pump beam is focused to a somewhat smaller waist than the probe.[34] The intensity at each data point is thus determined by a pulse-by-pulse normalization for the probe-laser detector current and pump-laser energy and then by averaging the normalized signal for (typically) 40 pump-laser pulses.

The measurements were made in an internally heated pressure vessel at pressures from 2 to 50 atm and at temperatures from 295 to 1000 K. The pump- and probe-laser beams cross inside the heated gas volume at a small angle (0.018 rad) at the focus of a 470-mm focal-length lens. The focused-beam diameters are approximately 100 μm. We measured the gas pressure in the vessel with strain-gauge transducers accurate to ± 0.2 atm at 50 atm, or with capacitance manometers accurate to ± 0.01 atm below 10 atm. Gas densities were calculated in amagat density units using expressions for virial coefficients including quantum deviations given in Ref. 35. A $\sim 3\%$ maximum deviation below ideal-gas density was found at 295 K and 50 atm.

Data were acquired from two different configurations of the heated section of the vessel because of suspected systematic temperature-measurement errors in the first configuration.[32] In this configuration, temperature was monitored with two thermocouples outside the surface of, but not in physical contact with, the heated 12.7-mm-i.d. ceramic cylinder core. One was located near the heater and the other near a small hole centered on the sample-gas volume which contained a 6-mm-i.d. molybdenum cylinder. Temperatures from fits to N_2 spectra measured in this configuration indicated gas temperatures up to $\sim 5\%$ higher than those measured by the gas-sample thermocouple. The furnace has now been rebuilt into a second configuration in which the molybdenum cylinder is removed and the second thermocouple tip has been brought into the gas volume. In this case, the heater thermocouple reads higher (up to 60 K at 1000 K) than the one in the sample-gas. Thus we suspect that any systematic error would be an overestimation of sample-gas temperature since its leads pass through a small hole in ceramic tube to which the heater is attached. We found remarkable consistency between measurements on the highly temperature-sensitive $Q(1)$ density-shift coefficients[32] in the two configurations. We have concluded that the upper limit for systematic errors in the earlier configuration (used for the linewidth data presented here) are actually less than 2.5%. The resulting estimate of errors in our temperature measurements are ± 5 K at 450 K, ± 15 K at 725 K, and ± 25 K at 1000 K. The room-temperature data were actually acquired at temperatures between 295 and 296 K. The actual temperature is used to calculated density, but the results are all quoted at 295 ± 1 K.

Besides the temperature- and density-measurement accuracies, a number of other experimental factors influence the accuracy of the broadening coefficients determined from these experiments. These factors include signal-to-noise ratio, peak signal level, ac Stark effects, optical alignment, and scan nonlinearities. In H_2 gas, because of the very large Raman cross section, it is possible to obtain an IRS signal that represents several percent peak absorption of the probe laser. If this is allowed, the signal is no longer linear in the imaginary part of $\chi^{(3)}$ and the line shape will be depressed at the peak,

causing a broader linewidth to be measured. We maintained the peak stimulated Raman absorption at less than 0.5% by attenuating the pump laser on strong transitions. The resulting systematic error in the linewidth is less than 0.25%. The optimum signal-to-noise ratio is then achieved by increasing the probe-laser power until the signal strength matches the dynamic range of the detection electronics. This occurs for a probe-detector current near 30 mA for our apparatus. For most of these measurements the probe laser was at 476.5 nm with a detector current of 28 mA. A spectrum, taken under these conditions, of the $J=2$ transition at 450 K and 50.7 atm is shown in Fig. 1(a) along with a fit to a Lorentzian profile. Taking the noise to be the rms deviation of the data from the fit, we find the peak signal-to-noise ratio to be 527. For these data, the primary limitation (other than density and temperature measurement accuracy) is the accuracy to which we can linearize the pump-laser frequency scan (discussed above).

For weaker transitions, the pump-laser energy was increased up to a maximum of 2.8 mJ or 126-kW peak power. At this power, an ac Stark shift of almost 0.002 cm^{-1} is observed.[32] An example of spectra taken at this power level is that of the $J=5$ transition shown in Fig. 1(b). The signal-to-noise ratio (as defined above) is only 130, but the uncertainties in the width due to optical-field inhomogeneities and the splitting of the orientational degeneracy[36] is probably greater than that due to the noise.

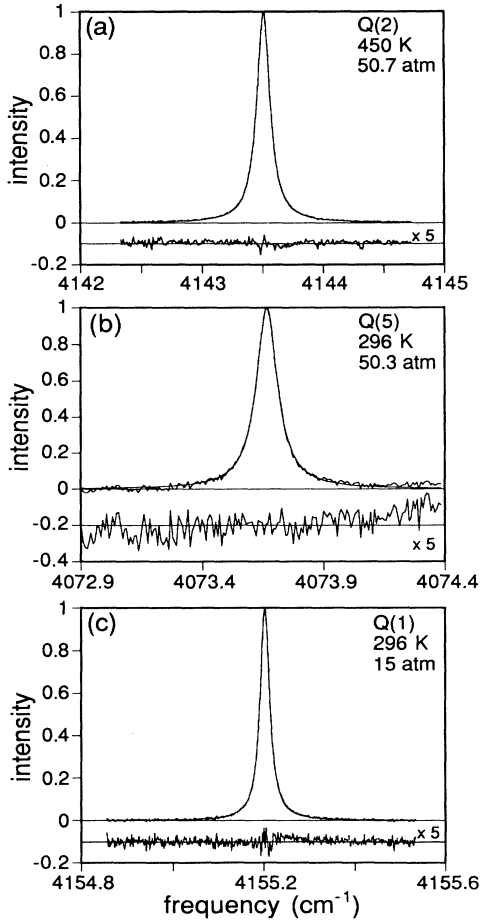

FIG. 1. Some examples of IRS spectra (solid lines) of Q-branch transitions and the associated Lorentzian fits (dashed lines). The residual (experiment minus fit) is plotted under each spectrum: (a) the $Q(2)$ spectrum measured at 450 K and 50.7 atm; (b) the $Q(5)$ spectrum measured at 295 K and 50.3 atm; (c) the $Q(1)$ spectrum measured at 295 K and 15.0 atm.

Careful alignment and focusing of the lasers was critical in eliminating two effects that adversely affected measured spectra. The first of these is the accuracy of the pump-laser energy normalization already described. When the pump-laser waist is too large or the laser has very large energy fluctuations, the signal-to-noise ratio is no longer quantum limited due to the presence of normalization noise that is proportional to the signal strength. An example of this is apparent in the residual shown below the spectra for the $J=1$ transition in Fig. 1(c). The second alignment-related problem occurs at high densities. We find that small asymmetries are easily observed in the line shape that depend on the overlap of the pump and probe laser foci and aperturing in the probe detection system. These effects are thought to be nonlinear refractive index (real part of $\chi^{(3)}$) phenomena which steer the probe beam and appear as attenuation of the beam when it is apertured by the detection system. With careful alignment and a nonaperturing detection system, the asymmetries disappear and the line shapes are highly Lorentzian.

III. EXPERIMENTAL RESULTS

The H_2 Q-branch line shape contains contributions from both the Doppler effect and collisional broadening. At very low pressures, the Doppler effect dominates and the line shape is Gaussian. At increasing pressures, the line is dramatically narrowed by phase-preserving velocity-changing collisions until collisional broadening causes the line to broaden again at higher pressures. The narrowing of the Doppler profile was first described by Dicke[1] and the theory was later extended to include collisional dephasing by Galatry[37] and Rautian and Sobel'man.[38] The dependence of the line shape on the collisional models of the latter two papers has been studied recently by Farrow and Palmer.[39] A Lorentzian line shape is predicted for pressures above that for which the velocity-changing collision rate greatly exceeds the Doppler width. In this "Dicke regime,"[1] valid for the data reported here, the line shape is Lorentzian having a half width at half maximum (HWHM) given in Hz by

$$\Gamma = 2\pi D_0 \nu_R^2 / c^2 \rho + \rho\gamma \ , \tag{1}$$

where D_0 is an optical diffusion coefficient, ν_R is the Raman frequency, c is the speed of light, ρ is the density, and γ is the collisional broadening coefficient. This expression assumes a collinear propagating geometry. We note that this, and all other equations in this report, are given in SI units. We will often report values for parameters, however, in more traditional units (e.g., D_0 in cm^2 amagat/s and γ in cm^{-1} amagat^{-1} where 1 amagat of $H_2 = 44.588\ 14$ mol/m^3).

The collisional broadening coefficients, shown in Table I, were determined from least-squares fits to a Lorentzian line shape of H_2 Q-branch lines measured at 50 atm. The linewidths were corrected for (small) Doppler contributions using Eq. (1). The application of this equation can lead to uncertainties in the values listed in Table I in addition to the experimental uncertainties already discussed. In particular, broadening coefficients derived from Eq. (1) depend on our knowledge of D_0 and its temperature dependence, and on the assumption that the collisional width is linear in density. While both of these issues are discussed below, we have found that neither contribute significantly to the uncertainties in our measurements. The estimated (2σ) errors (indicated in Table I) in the broadening coefficients reported here are due primarily to estimates of scan nonlinearities, Stark effects, and temperature-measurement uncertainties. We note, however, that a nonlinear density dependence *was* found[32] to be important in our earlier analysis of the density-shift data.

The optical diffusion coefficient for $Q(1)$ at 295 K has been measured[13,26,28] to be 1.35–1.42 cm^2 amagat/s. These results are very close to the mass diffusion coefficient calculated (1.33 cm^2 amagat/s) from the relations given by Hirschfelder, Curtiss, and Bird.[35] Bischel and Dyer[13] have reported, however, a temperature dependence, proportional to $T^{0.92}$, for the optical diffusion coefficient that is significantly higher than the $T^{0.72}$ expected[35] for the mass diffusion coefficient.

We have investigated this point by measuring the $Q(1)$ linewidth for densities from 2 to 45 amagat at 296 K and to 14 amagat at 1000 K. The results and fits to Eq. (1) are shown in Fig. 2. The best-fit values at 296 K are $D_0=1.55$ cm^2 amagat/s and $\gamma=0.871\times10^{-3}$ cm^{-1} amagat^{-1}. If we assume that a laser spectral width (HWHM) of 1.5×10^{-3} cm^{-1} may be subtracted in quadrature from the measured widths, an equally good fit (RMS error$=0.2\times10^{-3}$ cm^{-1}) is obtained with $D_0=1.42$ cm^2 amagat/s and $\gamma=0.870\times10^{-3}$ cm^{-1} amagat^{-1}. The sensitivity of the best-fit value of D_0 to the laser width is due to the extremely small width of the $Q(1)$ line at the Dicke minimum. At 1000 K the best-fit values are $D_0=3.67$ cm^2 amagat/s and $\gamma=4.28\times10^{-3}$ cm^{-1} amagat^{-1}. The best-fit D_0 is also significantly higher than the value calculated[35] ($D_0=3.24$ cm^2 amagat/s) for mass diffusion but is much less sensitive to the assumed laser width. We have assumed that D_0 is independent of J and have obtained values for other

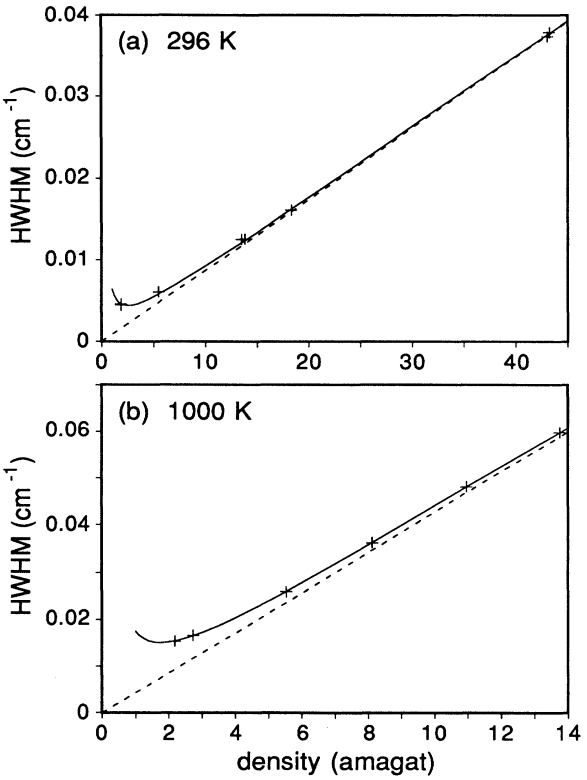

FIG. 2. The $Q(1)$ linewidth (HWHM) is plotted (symbols) vs the H_2 gas density at (a) 296 K and (b) 10 000 K. The solid lines are fits to Eq. (1).

temperatures by interpolating from the relation $D_0=0.01176T^{0.8314}$ derived from the 295-K theoretical and the 1000-K experimental values. At 50 atm, the Doppler correction is always less than 1% of the total width and, allowing a 10% error in D_0, the resulting uncertainties in γ are less than 0.1%.

The analysis of our data by Eq. (1) also assumes a linear dependence of γ on density. Moulton *et al.*[29] reported a nonlinear dependence above 1000 amagat for $Q(1)$ and $Q(2)$. The curvature in this data was described by a quadratic density term with a coefficient of 1.0×10^{-6} and 2.5×10^{-6} cm^{-1} amagat^{-2} for the HWHM of $Q(1)$ and $Q(2)$, respectively. While these authors comment that their $Q(1)$ measurements up to 800 amagat are consistent with a linear coefficient of

TABLE I. The density self-broadening coefficients from this work for the $Q(J)$ lines of H_2 at temperatures from 295 to 1000 K. The coefficients are in units of 10^{-3} cm^{-1} amagat^{-1}. The estimated errors are shown following each entry in the same units.

Q	296 K	450 K	725 K	1000 K
0	1.33±0.01	2.64±0.02	5.11±0.05	7.60±0.10
1	0.87±0.02	1.55±0.03	2.84±0.05	4.28±0.09
2	1.48±0.01	2.15±0.02	3.58±0.04	5.05±0.08
3	2.21±0.01	2.54±0.02	3.61±0.04	4.90±0.08
4	1.71±0.03	2.25±0.02	3.33±0.05	4.50±0.08
5	1.17±0.03	1.89±0.03	3.00±0.06	4.04±0.08

0.85×10^{-3} cm^{-1} $amagat^{-1}$, their quadratic fit yielded a linear coefficient of 0.65×10^{-4} cm^{-1} $amagat^{-1}$. The reported quadratic dependence would contribute 10–15 % to our measured widths at 45 amagat and 296 K. The data reported by Robert *et al.*[27] up to 100 amagat, Allin *et al.*[8] to 550 amagat, and that reported by May *et al.*[4] up to 800 amagat are also consistent with a linear density dependence. Robert *et al.*[27] have modeled the nonlinear density dependence of H_2 rare-gas broadening using a cubic term (with no quadriatic term) in accordance with the analysis of Royer.[40] Using a cubic rather than a quadratic density dependence to describe the high-density data of Moulton *et al.*[29] results in less than a 0.5% nonlinear-density contribution at 45 amagat. The $Q(1)$ broadening coefficient derived from our measurements at up to 45 amagat are in excellent agreement with other, even lower-density measurements[13,27,30] (see Table II). This agreement is taken as evidence that the quadratic density dependence of the linewidth is insignificant and we have not made nonlinear-density corrections to our linewidth data.

The previously reported values of the density-broadening coefficients in pure H_2 are compared with our measurements in Table II. The comparison included Raman and some electric-field-induced absorption measurements[9,41] at room temperature as well as, in the lower part of Table II, Raman measurements reported by Bischel and Dyer[13] at 450 K. We have omitted the results of Ref. 29 since these were discussed above. The data in Table II are chronologically ordered from right to left. The agreement of recent experiments with our results is very good. While the agreement with May *et al.*[4] and Hunt, Barnes, and Brannon[9] is also good, most of the other early work reports smaller broadening coefficients. The lower spectral resolution in many early experiments may have made it difficult to avoid systematic errors in linewidth measurements. For example, Murray and Javan[24] reported that they subtracted a constant instrumental resolution from their measured linewidths. Even at the highest densities, the resulting correction was 15–20 % of the measured widths. In cases such as this, deviations in the spectral shape of the instrument function, assumed to be Lorentzian in this case, towards a Gaussian shape can result in significant systematic errors that cause an underestimation of the broadening coefficients.

The $Q(1)$ broadening coefficient at 450 K attributed in Table II to Bischel and Dyer[13] was calculated from their best-fit formula [Eq. (2) of Ref. 13] describing the temperature dependence of the measured linewidth. This value is significantly lower than our measurement, as was their density-shift coefficient.[32] Both of these discrepancies can be resolved if we assume a systematic temperature-measurement error on their part of about +25 K (or −25 K on our part). We have investigated such a possibility in our experiments near 450 K with two different furnace geometries (described above) and find our results consistent with an uncertainty of ±5 K.

IV. ECS ANALYSIS

A. Contributions to collisional broadening of Raman transitions

Within the impact approximation[42] for isolated lines, collisions that result in modifications to the amplitude, phase, or frequency of Raman transitions will contribute to the broadening of the H_2 Raman spectrum. Inelastic collisions change the internal energy of the molecule, often changing the transition frequency and thereby completely dephasing the transition. Elastic collisions may induce transitions between degenerate orientational states and/or modify the phase of the transition *via* a transient frequency perturbation. As we have already mentioned, both elastic and inelastic collisional perturbations are infrequent for H_2 and the observed broadening can be approximated[10] as a sum of contributions from distinct collisional interactions.

We consider the contributions to isotropic, vibrational Q-branch transitions and, for later comparisons of rotationally inelastic rates, pure-rotational S-branch transitions. For the Q-branch transitions, the collisional broadening can be expressed as

$$\gamma_Q(v,J)=\gamma_{Q\phi}(v,J)+\gamma_{QJ}(v,J)\ , \tag{2}$$

where $\gamma_Q(v,J)$ is the (HWHM) collisional broadening coefficient from Eq. (1) for the $v\rightarrow v+1$ transition with rotational quantum number J, and $\gamma_{Q\phi}$ and γ_{QJ} are the

TABLE II. The density self-broadening coefficients (HWHM) from previous work are compared to those from this work for the $Q(J)$ lines of H_2 at 296 K to and near 450 K. The coefficients are in units of 10^{-3} cm^{-1} $amagat^{-1}$. The estimated errors are shown following each entry in the same units.

Q	This work	Ref. 30	Ref. 13	Ref. 28	Ref. 27	Ref. 26	Ref. 24	Ref. 41	Ref. 9	Ref. 8	Ref. 4
					296 K						
0	1.33±0.01	1.34±0.08	1.28±0.01	1.17			1.10±0.08	1.5	1.39±0.05	1.16±0.02	
1	0.87±0.02	0.90±0.05	0.87±0.02	0.84	0.83±0.05	0.86±0.01	0.75±0.05	1.05	0.92±0.05	0.70±0.02	0.95
2	1.48±0.01	1.51±0.08		1.26			1.3±0.1	1.8	1.52±0.05	1.26±0.02	
3	2.21±0.01	2.12±0.10		1.95			2.8±0.5	2.8	2.30±0.05	1.83±0.02	
4	1.71±0.03	1.66±0.10							1.63±0.05		
5	1.17±0.03	1.16±0.10									
					450 K						
1	1.55±0.03		1.44±0.03								

contributions from elastic vibrational dephasing,[43] and from rotational transfer out of level J, respectively. Broadening due to vibrationally inelastic collisions is assumed to be negligible. The inelastic broadening of the Q branch is related to the actual rotational transfer rate, $k_v(J \rightarrow J')$, from state (v,J) to state (v,J') by

$$\gamma_{QJ}(v,J)=\frac{1}{2\pi}\sum_{J\neq J'}\frac{k_v(J\rightarrow J')+k_{v+1}(J\rightarrow J')}{2} . \quad (3)$$

At room temperature and below, rotationally inelastic rates are sufficiently low that broadening by vibrational dephasing is a major contribution to the linewidth. For pure-rotational S-branch $(J\rightarrow J+2)$ transitions, the broadening coefficient is expressed as

$$\gamma_S(v,J)=\gamma_{SM}(v,J)+\gamma_{SJ}(v,J) , \quad (4)$$

where

$$\gamma_{SJ}(v,J)=\frac{1}{4\pi}\left[\sum_{J\neq J'}k_v(J\rightarrow J')+\sum_{J+2\neq J'}k_v(J+2\rightarrow J')\right] . \quad (5)$$

Here, $\gamma_{SM}(v,J)$ is the broadening contribution for S branches arising from elastic reorienting collisions that change the direction, but not the magnitude, of the molecular angular momentum vector $\mathbf{J}$.[44] This term does not appear in Eq. (2) because radiation arising from the isotropic polarizability is not dephased by changes in the orientation of $\mathbf{J}$.[6,44] In Eq. (4), we have neglected contributions from elastic rotational dephasing not involving reorientation.[44] If the vibrational state v dependences of the above processes are neglected, Eqs. (2) and (4) can be rewritten as

$$\gamma_Q(J)=\gamma_{Q\phi}(J)+\gamma_{QJ}(J) \quad (6)$$

and

$$\gamma_S(J)=\gamma_{SM}(J)+\tfrac{1}{2}[\gamma_{QJ}(J)+\gamma_{QJ}(J+2)] , \quad (7)$$

where

$$\gamma_{QJ}(J)=\frac{1}{2\pi}\sum_{J\neq J'}k(J\rightarrow J') . \quad (8)$$

Neglecting v dependence affects the comparison of our results with those of other experiments; this assumption will be examined in Sec. IV E below.

B. Rotational transfer rate models

Many phenomenological rate models (or fitting laws) have been developed to describe the rotational transfer rates of diatomic molecules. Several of these models have been developed for N_2 (Refs. 18 and 45) and CO (Ref. 20 and 21) based on extensive Raman Q-branch measurements of collisional broadening and narrowing. A modified-exponential-gap (MEG) model[18] has been used to model the rotational transfer rates in both HD (Refs. 15 and 46) and D_2.[14] An exponential gap model was also fit to measurements[47] of the H_2 rotational state-to-state rates in the $v=1$ state. While MEG models have not been applied to H_2 broadening coefficients, their successful application to the isotopes of H_2 suggests a similar approach for the present study.

One of the major difficulties with the MEG and other fitting laws is their inability to include explicitly resonances in the rotational energy-transfer rates due to collisions between molecules that are able to exchange rotational angular momentum with very little energy defect. Since H_2-H_2 collisions at moderate to low temperatures involve identical molecules in a few rotational levels, we would expect such resonant exchange collisions to play an important role. Keijser *et al.*[31] have estimated from room-temperature line-broadening studies that up to 40% of the pure-rotational $S(1)$ collision width results from resonant exchange collisions between molecules in the $J=1$ and $J=3$ levels.

The MEG analysis of D_2 by Smyth, Rosasco, and Hurst[14] resulted in rotational relaxation contributions from fits to linewidth data that compared favorably (particularly for self-broadening) to theory, as did the predicted magnitude of elastic dephasing. The D_2-He results from this study are also in good agreement with recent *ab initio* calculations.[16] The high-J collisional widths for D_2-H_2 were, however, larger than predicted by the best-fit model. This disagreement was attributed to the importance of nearly resonant exchange collisions. Hinchen and Hobbs[48] and Copeland and Crim[49] accounted for nearly and fully resonant exchange collisions in their analyses of HF self-broadening with an extended energy-gap model that included rotational level changes of the perturber molecules. Our attempts to analyze H_2 broadening using a similar energy-gap model gave unsatisfactory results, primarily, we believe, because the model does not allow independent variation of the magnitudes of contributions from resonant and nonresonant rotational energy-transfer processes.

The energy-corrected sudden (ECS) scaling theory of DePristo *et al.*[33,50] can be used to describe many collisional effects on line shapes, including broadening by rotationally and vibrationally inelastic collisions, elastic reorientational broadening, and collisional line shifts. The ECS theory provides quantum number scaling relationships among the elements of the scattering S matrix (and consequently, among the corresponding rates of collisional processes) by approximating certain exact properties of the S matrix. As a result, the scaling relationships for rotational transfer rates, along with microscopic reversibility, can be used to express an entire rate matrix in terms of a single row (or submatrix) of rates. These so-called basis rates are not provided by the ECS theory but can be determined experimentally, or calculated using detailed collision theory. Another alternative is to model the basis rates by using empirical expressions with adjustable parameters. The ECS theory, like the fitting laws, does not address broadening by elastic vibrational dephasing.

Thus, in contrast to simple energy-gap laws, ECS-based models incorporate justifiable quantum number scaling relationships and use fitting parameters (basis rates and scaling lengths) with specific dynamical meanings. The internal energy spacing of both the radiating and perturbing molecules can be taken into account, as well as the finite duration of the collisions. DePristo and

Rabitz[51] have demonstrated the applicability of the ECS formalism to *ab initio* calculations of R-T cross sections for the H_2-H_2 and HF-HF systems. The application of these models to experimental line-broadening measurements has been investigated for diatomic molecules such as HCl,[50] HF,[52] CO,[53] and N_2.[54] For these reasons and because of its simplicity we have used the ECS scaling theory to model the inelastic H_2-H_2 rates.

C. ECS modeling of H_2-H_2 collisional broadening

As previously discussed, we assume that contributions from distinct broadening processes (e.g., rotationally inelastic and elastic collisions) are simply additive. Neglecting v-level dependences in the rates, the Q-branch broadening coefficients are given by Eq. (6). Contributions from rotational transfer, $\gamma_{QJ}(J)$, are modeled using ECS scaling theory. The various models investigated for the elastic vibrational dephasing, $\gamma_{Q\phi}(J)$, are described at the end of this section.

Following DePristo *et al.*[33,50] the inelastic contributions are classified as either rotational-to-translational (R-T) or rotational-to-rotational (R-R) angular momentum transfer processes. If the radiating molecule angular momentum changes from J to J' and the perturber from K to K' then, R-R collisions are those that conserve rotational quanta ($J+K=J'+K'$) and R-T collisions are those that do not ($J+K\neq J'+K'$). Note that resonant exchange collisions are a subset of the R-R collisions ($J'=K$ and $K'=J$). The R-T contributions are modeled using an effective "atom-molecule" scaling expression, where the dynamical parameters are in effect averaged over initial and final levels of the perturber (DePristo, *et al.*[50] have shown that ΔJ changes in the perturber are not important in scaling R-T collisions of diatomic molecules):

$$k_{R\text{-}T}(J\to J')=(2J'+1)\exp[-\Delta(E_J,E_{J'})/kT]\Omega^2(J\to J',0\to 0)$$
$$\times\sum_L \begin{pmatrix} J & J' & L \\ 0 & 0 & 0 \end{pmatrix}^2 (2L+1)\Omega^{-2}(L\to 0,0\to 0)k_{R\text{-}T}(L\to 0),\quad J\neq J' . \tag{9}$$

Here, $k_{R\text{-}T}(J\to J')$ is the rotational transfer rate in terms of the basis rates $k_{R\text{-}T}(L\to 0)$, E_J is the rotational energy, ( ) denotes a 3-J symbol, and

$$\Delta(E_J,E_{J'})=\begin{cases} 0, & E_J>E_{J'} \\ E_{J'}-E_J, & E_J\leq E_{J'} \end{cases} \tag{10}$$

ensures microscopic reversibility. The finite duration of collisions is included through an adiabaticity factor

$$\Omega(J\to J',K\to K')$$
$$=\frac{1}{1+\omega^2(J\to J',K\to K')(b_c^{R\text{-}T})^2/24\bar{v}^2}, \tag{11}$$

where $b_c^{R\text{-}T}$ is the scaling length for R-T collisions (taken as an adjustable parameter), $\bar{v}=\sqrt{8kT/\pi\mu}$ is the mean relative molecular speed with μ the reduced collision mass, and

$$\omega(J\to J',K\to K')=(E_J+E_K-E_{J-\Delta J}-E_{K-\Delta K})/\hbar , \tag{12}$$

where ΔJ and ΔK are defined by

$$\Delta J=\begin{cases} 2(J-J')/|J-J'|, & J\neq J' \\ 0, & J=J' . \end{cases} \tag{13}$$

The basis rates are modeled using a simple energy-gap expression:

$$k_{R\text{-}T}(J\to 0)=\begin{cases} \alpha_{R\text{-}T}(T)\exp(-\beta E_J/kT) & \text{even } J \\ 0 & \text{otherwise} \end{cases} \tag{14}$$

where $\alpha_{R\text{-}T}(T)$ and β are adjustable parameters. This functional form was motivated by the success of the similar MEG model in describing the inelastic rates of D_2.[14]

The R-R rates are given by

$$k_{R\text{-}R}(J\to J',K\to K')=(2J'+1)(2K'+1)\exp[-\Delta(E_J+E_K,E_{J'}+E_{K'})/kT]\Omega^2(J\to J',K\to K')$$
$$\times\sum_{L,M}\begin{pmatrix} J & J' & L \\ 0 & 0 & 0 \end{pmatrix}^2\begin{pmatrix} K & K' & M \\ 0 & 0 & 0 \end{pmatrix}^2(2L+1)\Omega^{-2}(L\to 0,0\to M)$$
$$\times\exp[\Delta(E_L,E_K)]k_{R\text{-}R}(L\to 0,0\to M),\quad J+K=J'+K' , \tag{15}$$

where the adiabaticity parameters are given by Eq. (11) using a different scaling length, $b_c^{R\text{-}R}$. The basis rates are modeled by

$$k_{R\text{-}R}(L\rightarrow 0,0\rightarrow M)=\begin{cases}\alpha_{R\text{-}R}(T), & L=M=2\\ 0 \quad \text{otherwise} .\end{cases} \tag{16}$$

The use of a single R-R basis rate (at a given T) follows similar ECS analyses of HCl (Ref. 50) and CO (Ref. 53) collisional widths. Equation (16) neglects basis rates that are nonresonant ($L\neq M$) and those with $|\Delta L|>2$, the minimum quantum change. These assumptions constrain all R-R rates with $|\Delta J|$ or $|\Delta K|>2$ to be zero, but do not constrain nonbasis rates to be resonant. (We investigated the use of an additional resonant basis rate with $L=M=4$, but obtained a best-fit value of zero for this rate.)

The net rate of collisional transfer from J to J' for a radiating molecule is obtained from Eqs. (9)–(16) and

$$k(J\rightarrow J')=k_{R\text{-}T}(J\rightarrow J')+\sum_{K,K'=J-J'+K} n(K,T)\times k_{R\text{-}R}(J\rightarrow J',K\rightarrow K') , \tag{17}$$

where $n(K,T)$ is the fractional population of perturbers in level K, with $\sum_K n(K,T)=1$. The R-R rates are thus averaged over initial perturber levels. Note that the temperature dependence of the rates has been suppressed in this notation, but enters through the temperature-dependent parameters $\alpha_{R\text{-}T}(T)$, $\alpha_{R\text{-}R}(T)$, and the adiabaticity factor Ω (through $\bar{v}$). We compute net inelastic collisional broadening coefficients using Eq. (8).

We investigated three models for the elastic vibrational dephasing contributions to the collisional widths. The first, and simplest, follows the results of Smyth, Rosasco, and Hurst[14] for D_2, where $\gamma_{Q\phi}$ was assumed to be independent of J at room temperature. For scaling with temperature, we used

$$\gamma_{Q\phi}(J,T)=\left[\frac{T}{296}\right]\gamma_{Q\phi}^0 \quad \text{(model 1)} \tag{18}$$

(HWHM) in accordance with the calculations of Kelley and Bragg,[10] who found $\gamma_{Q\phi}(1,T)$ to be approximately proportional to T above 300 K. A single value for $\gamma_{Q\phi}^0$ for all J levels and temperatures was obtained from least-squares fitting.

The two remaining models were motivated by long-standing suggestions[10,9,55] that vibrational dephasing contributions to Q-branch widths in H_2 include a term proportional to rotational level population. This term is presumed to arise from a resonant coupling interaction.[10] The net elastic dephasing is thus assumed to be

$$\gamma_{Q\phi}(J,T)=\gamma_{Q\phi}^0(T)+\gamma_{Q\phi}^1(T)n(J,T) \quad \text{(model 2)} , \tag{19}$$

where the first term is a J-independent contribution. While fitting data with this expression, we found that the magnitude of $\gamma_{Q\phi}^1$ at 296 K was not well determined due to a strong correlation with the ECS fitting parameters. Consequently, we used experimentally determined rotational transfer rates[47,56,57] to fix a value for $\gamma_{Q\phi}^1$ at 296 K that was consistent with the observed linewidths for $J=1$ and $J=3$. The value was obtained using Eqs. (7), (8), and (19) and assuming a two-level system, yielding two relations for the collisional widths in terms of the transfer rates between these levels and the parameters describing elastic dephasing:

$$\gamma_Q(1)\cong k(1\rightarrow 3)/2\pi+\gamma_{Q\phi}^0+\gamma_{Q\phi}^1 n(1)$$

and

$$\gamma_Q(3)\cong k(3\rightarrow 1)/2\pi+\gamma_{Q\phi}^0+\gamma_{Q\phi}^1 n(3) .$$

These two relations were solved using widths from Table I, and the rates $k(1\rightarrow 3)/2\pi=0.29\times 10^{-3}$ $\text{cm}^{-1}\,\text{amagat}^{-1}$ from experiment[47,56,57] and $k(3\rightarrow 1)/2\pi=2.04\times 10^{-3}$ $\text{cm}^{-1}\,\text{amagat}^{-1}$ from microscopic reversibility. The resulting parameters were $\gamma_{Q\phi}^0(296\text{ K})=0.104\times 10^{-3}$ $\text{cm}^{-1}\,\text{amagat}^{-1}$ and $\gamma_{Q\phi}^1(296\text{ K})=0.72\times 10^{-3}$ $\text{cm}^{-1}\,\text{amagat}^{-1}$. The latter result is comparable to that of Bischel and Dyer,[13] 0.75×10^{-3} $\text{cm}^{-1}\,\text{amagat}^{-1}$, and that of Gray and Welsh,[55] 0.70×10^{-3} $\text{cm}^{-1}\,\text{amagat}^{-1}$, both at 298 K. For the fits at 296 K, $\gamma_{Q\phi}^1$ was held fixed and $\gamma_{Q\phi}^0$ was varied, while, at all other temperatures, both coefficients in Eq. (19) were varied for best fit.

A third dephasing model, intermediate between models 1 and 2 in its prediction of J-dependent dephasing, was obtained by again using Eq. (19) but fixing the magnitude of the population term to that reported by Bischel and Dyer[13] for 81 K:

$$\gamma_{Q\phi}(J,T)=\gamma_{Q\phi}^0(T)+\gamma_{Q\phi}^1(81\text{ K})n(J,T) \quad \text{(model 3)} , \tag{20}$$

where $\gamma_{Q\phi}^1(81\text{ K})=0.42\times 10^{-3}$ $\text{cm}^{-1}\,\text{amagat}^{-1}$. The magnitude of the J-independent term $\gamma_{Q\phi}^0(T)$ was varied for best fit. The population coefficient was assumed to be independent of temperature for simplicity.

D. ECS fitting procedures and results

We used a FORTRAN computer program based on the freely available subroutine STEPIT (Ref. 58) to perform a nonlinear least-squares fitting of model predictions to the 24 collision broadening coefficients given in Table I. The coefficients, expressed in $\text{cm}^{-1}\,\text{amagat}^{-1}$, were multiplied by $273.15/T$ in the computations, equivalent to expressing them in units of cm^{-1} per ideal-gas atmosphere, so that low- and high-temperature magnitudes were comparable, and unweighted residuals were used. For the ECS modeling of the inelastic broadening, we varied the basis-rate magnitude parameters $\alpha_{R\text{-}T}(T)$ and $\alpha_{R\text{-}R}(T)$ for best fit at each temperature. A single value was varied for the basis-rate exponential factor β and for the scaling length $b_c=b_c^{R\text{-}T}=b_c^{R\text{-}R}$. (We judged that the fit sensitivity did not justify using separate R-T and R-R scaling lengths; this decision is discussed below.) In total, we varied ten parameters to model the inelastic rates. To model the elastic dephasing contributions, the number of additional parameters varied was 1 for model 1, 7 for model 2, and 4 for model 3.

The best-fit broadening coefficients predicted using dephasing model 1 are compared with the experimental results in Fig. 3. (Note that the coefficients from Table I have been multiplied by $273.15/T$ and are plotted in units of 10^{-3} $cm^{-1}atm^{-1}$.) The average deviation between measurements and model predictions is 1.0%, and is comparable to the experimental uncertainties. The model parameters for this fit are given in Table III. The horizontal dotted line in Fig. 3 indicates the best-fit vibrational dephasing contribution used at all J levels and temperatures. For this model, after multiplying by $273.15/T$, the dephasing coefficient is independent of temperature. The resulting coefficient, 1.32 $cm^{-1}amagat^{-1}$, compares favorably to results of other workers for 295–298 K (see Table IV). We investigated a possible temperature dependence in the dephasing contribution by varying its magnitude for best fit at each temperature. The resulting temperature-dependent values varied less than 10%, and the fits were not significantly improved.

The broadening contributions from R-T and R-R inelastic processes predicted by model 1 are shown in Figs. 4(a) and 4(b), respectively. The results indicate that R-R processes dominate the inelastic broadening for $J>0$ and $T<725$ K. At the two lower temperatures, especially 296 K, the R-R contributions are strongly peaked at $J=3$. At higher temperatures, the distribution broadens and moves to higher J, staying above the most highly populated J level. In addition, the R-R broadening becomes significantly less J dependent. This behavior arises mostly from the influence of resonant R-R collisions, as shown by the following argument. For $T\leq 450$, a majority of molecules are in the $J=1$ level. $J=3$ molecules, being the only colliders capable of resonant collisions with $J=1$ (due to nuclear-spin conservation and the neglect of R-R processes with $\Delta J>2$) exhibit enhanced broadening. If we assume that J-dependent R-R inelastic rates are proportional to the populations of resonant colliders, then broadening contributions for $J=0$, 1, 2, and 3 would have the approximate proportions $n(2):n(3):n(0):n(1)=0.12:0.09:0.13:0.66$ at 296 K, respectively. This is not unlike what is observed in Fig. 4(b). At higher temperatures, the distribution of resonant colliders would become smoother and move to higher J, also similar to the model results.

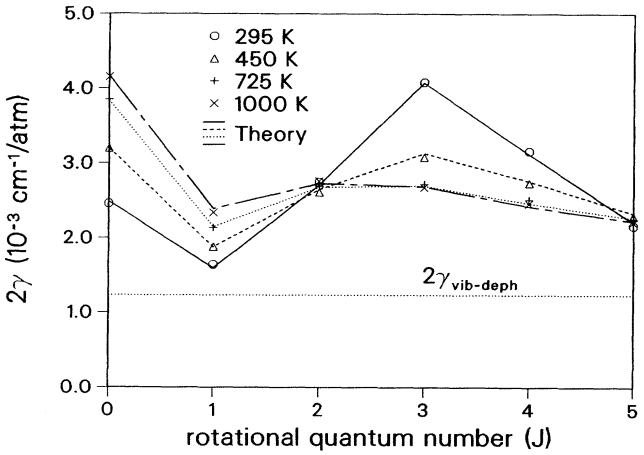

FIG. 3. Comparison of collisional broadening coefficients (symbols) measured with inverse Raman spectroscopy and ECS-based model predictions (lines) for Q-branch transitions in pure H_2. The calculations were fitted to the data using ECS scaling theory to model broadening by rotationally inelastic processes (R-T and R-R). Broadening by elastic vibrational dephasing was assumed to be additive with the inelastic broadening. Three different models for elastic dephasing contributions were tested: model 1 used a single coefficient, independent of temperature and rotational level, and is illustrated by the horizontal dotted line. The other models gave agreement matching that in the figure, and therefore are not shown.

TABLE III. Best-fit parameters for elastic-dephasing model 1 and the ECS model, given in units of 10^{-3} $cm^{-1}amagat^{-1}$.

	Temperature (K)			
Parameter[a]	296	450	725	1000
$\alpha_{R\text{-}T}$	18.6	8.16	4.96	4.31
$\alpha_{R\text{-}R}$	2.36	2.33	2.52	2.54
$\gamma^0_{Q\phi}$	0.66	0.66[b]	0.66[b]	0.66[b]

[a]For the temperature-independent ECS parameters we obtained $\beta=2.36$ and $b_c=1.77$ Å.
[b]This parameter was assumed to be independent of temperature for model 1.

The best-fit value for the effective scaling length b_c obtained with this model was 1.77 Å. Appearing in the adiabaticity factor [Eq. (11)], b_c is the only adjustable parameter affecting the scaling relationships, and is an indication of the spatial range of rotationally inelastic coupling. DePristo and Rabitz[51] have discussed the separation of R-T and R-R processes in the ECS formalism and reported a scaling length for calculated H_2-H_2 R-T cross sections of $0.8\ \text{Å}<b_c^{R\text{-}T}<1.3$ Å. Calculated cross sections for R-R processes were not available and were assumed to be small. In comparison, for CO Belbruno, Gelfand, and Rabitz[53] obtained $b_c^{R\text{-}T}=0.65\pm0.16$ Å and $b_c^{R\text{-}R}=0.4\pm0.1$ Å; however, the data did not provide sufficient sensitivity to accurately characterize the R-R interactions. For N_2 Bonamy *et al.*[54] obtained $b_c^{R\text{-}T}=0.75\pm0.05$ Å, but they did not model R-R processes explicitly. Since our result for a combined b_c was significantly larger than all of these values, we examined the effect of using two separately varied scaling lengths. In fitting data at 450 K and lower (where R-R processes dominate in H_2) we found that $b_c^{R\text{-}R}$ was sensitively determined to be near the value found earlier. However, the corresponding R-T scaling length was not well determined: good fits were obtained for values between 0.65 and 1.8 Å. This range is consistent with the results reported in Ref. 51. We conclude that our results do not provide sufficient sensitivity to establish separate scaling lengths, and that the combined value we obtain is largely representative of R-R interactions. It should be noted that this result is dependent on the elastic dephasing model used, and varies as low as 1.2 Å for model 2 (see Table V).

TABLE IV. Comparison of reported elastic vibrational dephasing contributions to the $Q(1)$ collision broadening coefficient at temperatures of 295–298 K, given in units of 10^{-3} cm^{-1} amagat^{-1}.

Source	Experiment	$2\gamma_{Q\phi}$
This work		
model 1		1.32
model 2	Line-broadening measurement	1.19
model 3		1.31
Ref. 10, 295 K	Semiclassical calculation	1.55
Ref. 47, 295 K	Energy transfer measurement	1.2±0.3
Ref. 13, 298 K	Line broadening measurement	1.0±0.1

The total broadening predictions obtained with dephasing models 2 and 3 are very similar to those obtained with model 1 (Fig. 3) and agree equally well with the data; thus, they are not shown. However, the different dephasing contributions of models 2 and 3 force a different partitioning of the linewidth among the three broadening processes, particularly at 295 and 450 K (see Tables V and VI). As seen in Figs. 5 and 6, the best-fit pure-dephasing contribution to $Q(1)$ is nearly independent of dephasing model and temperature. Other transitions have smaller contributions, dependent on their level populations and on the size of the J-independent dephasing term. The decreased elastic contributions with respect to model 1 are made up by increased inelastic broadening, with R-T contributions generally receiving the greatest percentage increase. To summarize, at the lower temperatures models 2 and 3 predict less elastic and greater inelastic broadening than model 1, except for the $Q(1)$ transition.

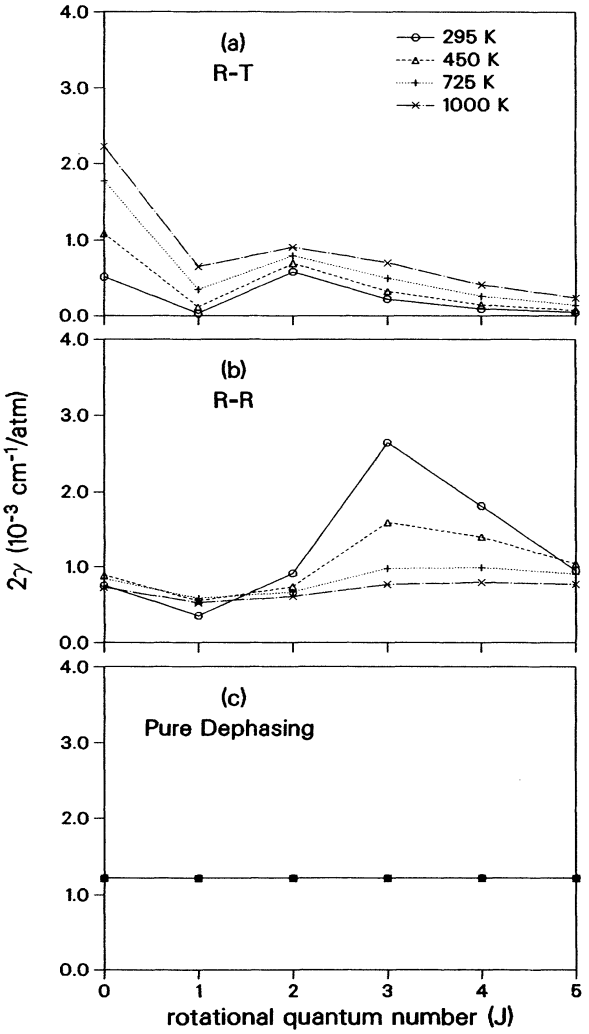

FIG. 4. Individual contributions to broadening coefficients (symbols) predicted using elastic dephasing model 1. (The lines are drawn connecting the symbols.) The inelastic R-T and R-R contributions were calculated using a model based on ECS scaling theory. Because the inelastic and elastic contributions were added and varied for best fit, the inelastic results are influenced by the elastic dephasing model.

We find that all three models are in close agreement at 725 and 1000 K because all use similar, nearly J-independent dephasing at these temperatures [see Figs. 4(c), 5(c), and 6(c)]. The explanation for this result differs for each model. J-independent dephasing was assumed in model 1. In model 2 the best-fit population-dependent dephasing term was found to be small compared to the J-independent term at high temperatures. This occurred because the smooth J dependence observed in the linewidths was incompatible with a 3:1 alternation in population arising from nuclear-spin degeneracies. In model 3 the population coefficient has an assumed value of 3.1×10^{-4} cm^{-1} atm^{-1} at 725 K and is even smaller at 1000 K. When multiplied by level populations, the resulting terms are small compared to the J-independent dephasing.

TABLE V. Best-fit parameters for elastic-dephasing model 2 and the ECS model, given in units of 10^{-3} cm^{-1} amagat^{-1}.

	Temperature (K)			
Parameter[a]	296	450	725	1000
$\alpha_{R\text{-}T}$	105.9	20.1	8.20	6.31
$\alpha_{R\text{-}R}$	2.50	2.21	1.91	1.74
$\gamma^0_{Q\phi}$	0.119	0.61	1.46	2.14
$\gamma^1_{Q\phi}$	0.72[b]	0.58	0.206	0.0

[a]For the temperature-independent ECS parameters we obtained $\beta=2.92$ and $b_c=1.20$ Å.

[b]Not fitted, but chosen to be consistent with experimental collision widths and rotational relaxation rates.

E. Comparison with other results

It is evident that, while there is good agreement (see Table IV) among the ECS-model predictions and other experiments and calculations for $Q(1)$ at room temperature, there are ambiguities in distinguishing elastic and inelastic broadening for the other transitions at the lower temperatures that cannot be resolved solely from our results. Fortunately, results that relate to other Q-branch transitions are available from numerous experimental and theoretical line-broadening and energy-transfer investigations reported for H_2 at room temperature. We now turn to comparisons of these results with predictions of the present models.

Several direct measurements of rotational transfer rates have been reported for H_2 in the $v=1$ level, with all in good agreement.[47,56,57] Figure 7 shows a comparison of rotationally inelastic contributions to the Q-branch broadening coefficients at ~296 K. The triangles indi-

TABLE VI. Best-fit parameters for elastic-dephasing model 3 and the ECS model, given in units of 10^{-3} cm^{-1} $amagat^{-1}$.

	Temperature (K)			
Parameter[a]	296	450	725	1000
$\alpha_{R\text{-}T}$	170.7	30.6	10.9	7.68
$\alpha_{R\text{-}R}$	2.45	2.37	2.54	2.47
$\gamma^0_{Q\phi}$	0.38	0.73	1.32	1.98
$\gamma^1_{Q\phi}$	0.42[b]	0.42[b]	0.42[b]	0.42[b]

[a]For the temperature-independent ECS parameters we obtained $\beta=3.38$ and $b_c=1.42$ Å.

[b]Not fitted, but chosen to agree with experimental results at 81 K reported by Bischel and Dyer (Ref. 13) and assumed to be temperature independent.

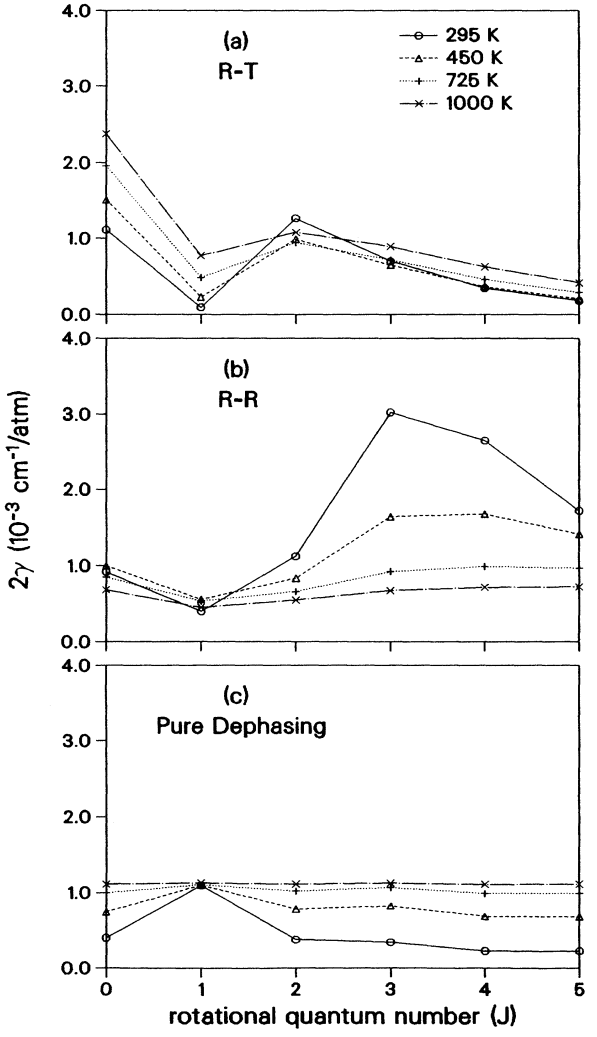

FIG. 5. Individual contributions to broadening coefficients (symbols) predicted using elastic dephasing model 2. (The lines are drawn connecting the symbols.)

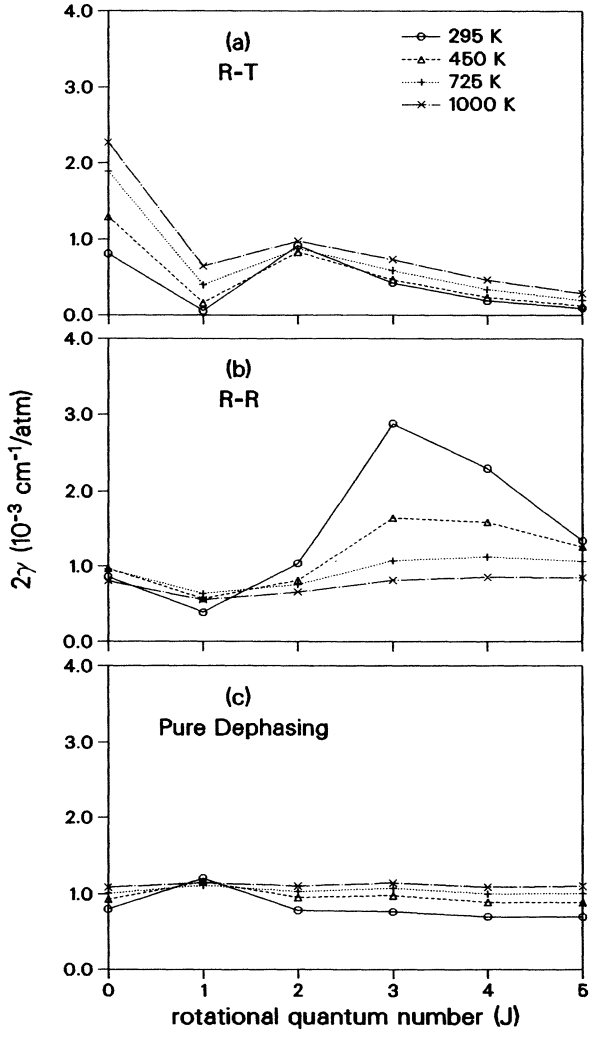

FIG. 6. Individual contributions to broadening coefficients (symbols) predicted using elastic dephasing model 3. (The lines are drawn connecting the symbols.)

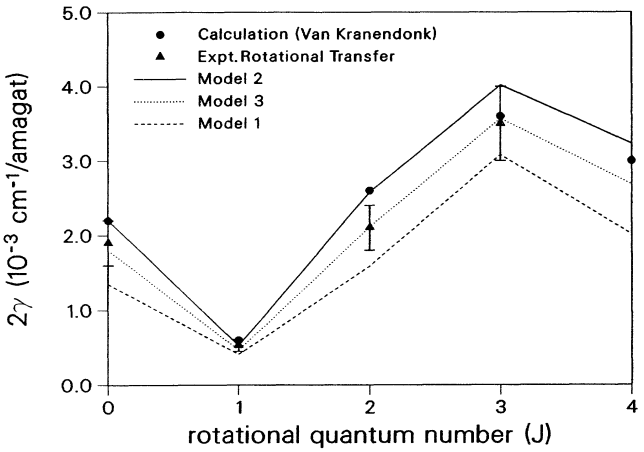

FIG. 7. Rotationally inelastic contributions to the Q-branch broadening coefficients of H_2 at room temperature. The solid circles indicate results calculated by Van Kranendonk (Ref. 6). The triangles indicate results based on experimental rotational transfer rates (Refs. 47, 56, and 57) computed using Eq. (8). The lines connect the results of models from this work.

cate contributions from experimental rotational relaxation rates for $v=1$ from Farrow and Chandler,[47] expressed using Eq. (8). The straight lines connect the net inelastic broadening predictions (R-$T+R$-R) of models 1–3. While none of the models clearly disagrees with the experimental rates, model 3 obviously exhibits the best agreement. We note, however, that the consideration of v dependences in the inelastic rates can significantly affect such comparisons. Due to experimental reasons, the transfer rates from Ref. 47 were measured in $v=1$, yet the inelastic Q-branch broadening results from an average of rates in $v=0$ and 1 [Eq. (3)]. Excited-state rates 10–30% higher than those in the ground state have been suggested by Rosasco *et al.*[15] for HD. Blackmore, Green, and Monchick[16] also found that their *ab initio* calculated inelastic rotational rates for D_2-He were ~30% higher for $v=1$ than for $v=0$. Such a v dependence would cause the corresponding linewidths to be up to ~15% smaller than those computed from the $v=1$ rates alone. This would result in closer agreement between the experimental rates (triangles in Fig. 7) and model 1.

The solid circles in Fig. 7 show results of the Anderson-type[56] scattering calculation by Van Kranendonk[6] referred to previously. It was the comparison of these results with observed linewidths that had initially motivated the population-dependent elastic dephasing models. Thus, it is not surprising that the best agreement is observed with model 2, which includes the largest population-dependent term. Keijser *et al.*[31] examined the ability of this theory to predict pure-rotational Raman linewidths. They found that adjustments in the resonance parameter of the theory were needed to correctly model the contributions of resonant R-R collisions; these were generally reduced by up to 50%. A similar reduction in the calculated Q-branch widths of Fig. 7 would produce better agreement with models 1 and 3. In contrast, Hunt, Barnes, and Brannon[9] included v dependencies in the theory by employing effective rotational constants, and found that the Q-branch widths *increased* by an average of 17% (using the resonance factor of Van Kranendonk). Clearly, more detailed calculations are required before this approach can be used to quantitively distinguish among sources of broadening.

A comparison of the model predictions with other results of Keijser *et al.*[31] proved more fruitful. We used Eqs. (7) and (8) and the rotational transfer rates to predict the *inelastic* contributions to pure-rotational linewidths. [For $S(J)$ this contribution is simply the average of the net relaxation rates out of levels J and $J+2$.] These results are compared in Fig. 8 to experimental and theoretical results from Ref. 31. Note that the experimental S-branch linewidths (indicated by solid circles) exceed the ground-vibrational-state inelastic rates since the former include additional broadening by elastic reorienting collisions. If we subtract the reorientational contributions calculated by Keijser *et al.*[31] (using the Van Kranendonk theory) from the observed linewidths, we obtain the purely inelastic contributions indicated by triangles in Fig.8. Even if these inelastic contributions are increased by ~15% to account for a possible v dependence, model 2 still lies significantly above the resulting total linewidth for $S(2)$ and $S(3)$. This is a result of the relatively large inelastic rates inherent in this model, arising from its use of smaller vibrational dephasing contributions to fit the Q-branch linewidths above $J=1$. Model 1 clearly exhibits the best agreement with these calculated ground-state inelastic rates, while a significant v dependence would bring model 3 into closer agreement. Model 2 is in significant disagreement.

Figure 9 shows a comparison of S-branch R-R contri-

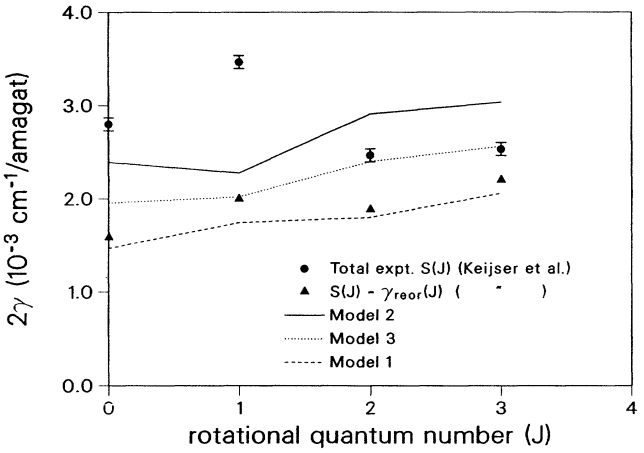

FIG. 8. Experimental broadening coefficients for pure-rotational transitions of H_2 at room temperature (solid circles), inelastic contributions (triangles) obtained from the experimental coefficients by subtracting elastic reorientational contributions obtained from theory, and inelastic contributions predicted by models from this work (lines). The experimental linewidths contain additional broadening contributions from elastic reorienting collisions, and therefore should be an upper limit for the inelastic model results.

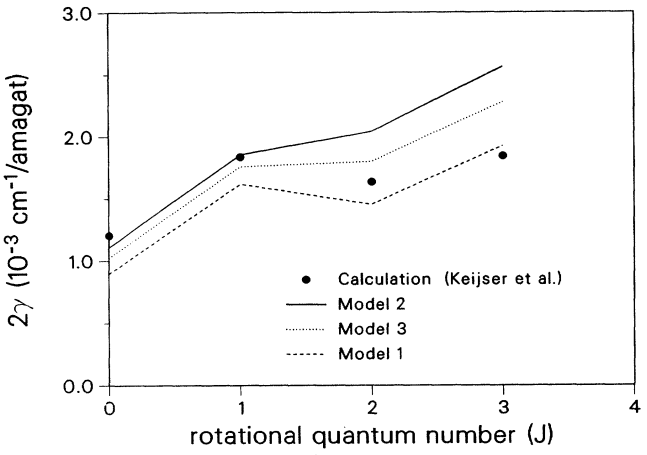

FIG. 9. Theoretical R-R broadening contributions for pure-rotational transitions of H_2 at room temperature (solid circles) obtained by Keijser *et al.* (Ref. 31) and R-R contributions predicted by models from this work.

butions from the models (lines) with theoretical R-R results by Keijser *et al.*[31] (solid circles). The latter were computed by adding the contributions for resonance and quasiresonance collisions given in Table VI of Ref. 31 and weighting the results for normal H_2. The model results were expressed as before for S branches. Good agreement in both J dependences and magnitudes is observed between theory and the results of models 1 and 3, supporting the validity of the ECS scaling of R-R collision rates. We consider the Keijser results to be partially grounded in experiment as they were adjusted to agree with measurements sensitive to R-R contributions (line-broadening measurements conducted with varying ortho/para composition). Note that considering higher inelastic rates in $v=1$ compared to $v=0$ would affect the magnitudes of the predictions of model 2, but its J dependence would continue to disagree with theory.

We also note that calculations[59-60] have been made of R-T cross sections for the H_2-H_2 system. The dominant rate in the calculation for parahydrogen by Rabitz and Lam[58] was for $J=0$, $J'=2$, and $K-K'=0$. The thermally (300 K) averaged[56] rate for parahydrogen collision partners would give rise to a $Q(0)$ broadening contribution of $k_{R\text{-}T}(0\rightarrow 2)/2\pi = 0.142\times 10^{-3}$ cm^{-1} $amagat^{-1}$. For comparison, the rates predicted by our models vary from 0.266×10^{-3} cm^{-1} $amagat^{-1}$ by model 1 to over twice that by model 2. Meier, Ahlers, and Zacharias[56] also reported a thermal average of the $k_{R\text{-}T}(1\rightarrow 3)$ cross sections reported by Zarur and Rabitz.[59] The contribution of this rate to the $Q(1)$ width would be small, $k_{R\text{-}T}(1\rightarrow 3)/2\pi = 0.044\times 10^{-3}$ cm^{-1} $amagat^{-1}$. The corresponding model predictions range from 0.048×10^{-3} cm^{-1} $amagat^{-1}$ for model 2 to less than $\frac{1}{3}$ that for model 1. Given the variations in the predictions of our models and the uncertainties associated with the calculations and the possible v dependencies, we consider the agreement to be good.

V. SUMMARY AND CONCLUSIONS

In summary, ECS scaling theory was used to model rotationally inelastic contributions to self-broadening measurements of the first six Q-branch transitions of H_2 from 295 to 1000 K. Because of the importance of broadening by elastic vibrational dephasing, we investigated three different models for this contribution. The total linewidth predicted by all these models was in excellent agreement with our data, and the detailed broadening contributions predicted by the models were similar at high temperatures. At lower temperatures the models disagreed in the partitioning of broadening between elastic and inelastic processes. In all cases, the elastic broadening per unit pressure of $Q(1)$ was found to be nearly independent of temperature. Comparisons of the models with other room-temperature linewidth measurements and theory, and with experimental rotational transfer measurements were fruitful: a model with J-independent elastic dephasing or one with a small population-dependent elastic term were preferred. The agreement with the derived ground-state inelastic rates was best for model 1. Model 3 predicts inelastic rates that are about 15% higher than for model 1 and that are in good agreement with the experimental $v=1$ rates. Thus the available experimental information on inelastic rates, shown in Fig. 7 and 8, indicates that the rotationally inelastic rates in $v=1$ are approximately 15% higher than those of $v=0$. These results suggest that a model with a population-dependent dephasing between that of models 1 and 3 would provide the best overall agreement with both the linewidth and inelastic-rate measurements made to date. The $\sim 15\%$ v dependence inferred here for H_2-H_2 is consistent with, but somewhat lower than, that inferred for the HD-HD system.[15] This v dependence is also considerably less, however, than that predicted by the rather convincing calculations reported in Ref. 16 on the D_2-He system (see Table I of the second paper of Ref. 16). The D_2-He system is dominated by very short-range collisions and the rotational inelasticity is due entirely to R-T processes. Detailed calculations such as these on systems like H_2-H_2, where R-R processes dominate, would be very interesting.

We have shown ECS scaling theory to be a powerful tool for distinguishing R-T and R-R line-broadening processes in pure H_2. Unlike many energy-gap laws, ECS models are derived from physical considerations of scattering S matrices. Our results corroborate the importance of R-R processes in H_2 line broadening indicated in previous studies. To facilitate quantitative comparisons among various line-broadening and energy-transfer experiments, more work is needed for addressing the question of v dependences in the energy-transfer rates.

ACKNOWLEDGMENTS

The authors would like to acknowledge useful discussions with J. D. Kelly, and the expert technical assistance provided by Steve Gray in performing these experiments. This work was supported by the U.S. Department of Energy, Office of Basic Energy Sciences, Chemical Sciences Division, and by the U.S. Army Research Office.

[1]R. H. Dicke, Phys. Rev. **89**, 472 (1953).
[2]R. G. Gordon, J. Chem. Phys. **45**, 1649 (1966).
[3]R. L. Farrow, L. A. Rahn, G. O. Sitz, and G. J. Rosasco, Phys. Rev. Lett. **63**, 746 (1989).
[4]A. D. May, V. Degen, J. C. Stryland, and H. L. Welsh, Can. J. Phys. **39**, 1769 (1961).
[5]A. D. May, G. Varghese, J. C. Stryland, and H. L. Welsh, Can. J. Phys. **42**, 1058 (1964).
[6]J. Van Kranendonk, Can. J. Phys. **41**, 433 (1963).
[7]P. W. Anderson, Phys. Rev. **76**, 647 (1949).
[8]E. J. Allin, A. D. May, B. P. Stoicheff, J. C. Stryland, and H. L. Welsh, Appl. Opt. **6**, 1597 (1967).
[9]R. H. Hunt, W. L. Barnes, and P. J. Brannon, Phys. Rev. A **1**, 1570 (1970).
[10]J. D. Kelley and S. L. Bragg, Phys. Rev. A **34**, 3003 (1986).
[11]P. Lallemand and P. Simova, J. Mol. Spectrosc. **26**, 262 (1968).
[12]E. C. Looi, J. C. Stryland, and H. L. Welsh, Can. J. Phys. **56**, 1102 (1978).
[13]W. K. Bischel and M. J. Dyer, Phys. Rev. A **33**, 3113 (1986).
[14]K. C. Smyth, G. J. Rosasco, and W. S. Hurst, J. Chem. Phys. **87**, 1001 (1987).
[15]G. J. Rosasco, A. D. May, W. S. Hurst, L. B. Petway, and K. C. Smyth, J. Chem. Phys. **90**, 2115 (1989).
[16]R. Blackmore, S. Green, and L. Monchick, J. Chem. Phys. **88**, 4113 (1988); S. Green, R. Blackmore, and L. Monchick *ibid.* **91**, 52 (1989).
[17]T. A. Brunner and D. Pritchard, in *Dynamics of the Excited State,* edited by K. P. Lawley (Wiley, New York, 1982), pp. 589–641.
[18]L. A. Rahn and R. E. Palmer, J. Opt. Soc. B **3**, 1164 (1986).
[19]M. L. Koszykowski, L. A. Rahn, R. E. Palmer, and M. E. Coltrin, J. Phys. Chem. **91**, 41 (1987).
[20]G. J. Rosasco, L. A. Rahn, W. S. Hurst, R. E. Palmer, and S. M. Dohne, J. Chem. Phys. **90**, 8 (1989).
[21]J. P. Looney, G. J. Rosasco, L. A. Rahn, W. S. Hurst, and J. W. Hahn, Chem. Phys. Lett. **161**, 232 (1989).
[22]P. Lallemand, P. Simova, and G. Brett, Phys. Rev. Lett. **17**, 1239 (1966).
[23]J. R. Murray and A. Javan, J. Mol. Spectrosc. **29**, 502 (1969).
[24]J. R. Murray and A. Javan, J. Mol. Spectrosc. **42**, 1 (1972).
[25]F. DeMartini, F. Simoni, and E. Santamato, Opt. Commun. **9**, 176 (1973).
[26]A. Owyoung, Opt. Lett. **2**, 91 (1978).
[27]D. Robert, J. Bonamy, J. P. Sala, G. Levi, and F. Marsault-Herail, Chem. Phys. **99**, 303 (1985).
[28]A. M. Toich, D. W. Melton, and W. B. Roh, Opt. Commun. **55**, 406 (1985).
[29]N. E. Moulton, G. H. Watson, Jr., W. B. Daniels, and D. M. Brown, Phys. Rev. A **37**, 2475 (1988).
[30]R. L. Farrow and G. O. Sitz, J. Opt. Soc. Am. **6**, 865 (1989).
[31]R. A. J. Keijser, J. R. Lombardi, K. D. Van Den Hout, B. C. Sanctuary, and H. F. P. Knapp, Physica **76**, 585 (1974).
[32]L. A. Rahn and G. J. Rosasco, Phys. Rev. A **41**, 3698 (1990).
[33]A. D. DePristo, J. Chem. Phys. **73**, 2145 (1980).
[34]L. A. Rahn, Opt. Lett. **7**, 66 (1982); for corrections in the equations of this paper, see L. A. Rahn, Sandia National Laboratory Report No. SAND81-8807, 1982 (unpublished).
[35]J. O. Hirschfelder, C. F. Curtiss, and R. B. Bird, *Molecular Theory of Gases and Liquids* (Wiley, New York, 1964).
[36]H. Moosmuller, C. Y. She, and Winifred M. Huo, Phys. Rev. A **40**, 6983 (1989).
[37]L. Galatry, Phys. Rev. **122**, 1258 (1961).
[38]S. G. Rautian and I. I. Sobel'man, Usp. Fiz. Nauk **90**, 209 (1966) [Sov. Phys. Usp. **9**, 701 (1967)].
[39]R. L. Farrow and R. E. Palmer, Opt. Lett. **12**, 984 (1987).
[40]A. Royer, Phys. Rev. A **22**, 1625 (1980).
[41]H. L. Buijs and H. P. Gush, J. Phys. **49**, 2366 (1971).
[42]A. Ben-Reuven, in *Advances in Chemical Physics,* edited by I. Prigogine and Stuart A. Rice (Wiley, New York, 1975), Vol. 33, pp. 235–293.
[43]F. Marsault-Herail, G. Levi, and J. P. Marsault, Chem. Phys. Lett. **74**, 467 (1980).
[44]R. G. Gordon, J. Chem. Phys. **44**, 3083 (1966).
[45]D. A. Greenhalgh, in *Adavances in Non-Linear Spectroscopy* edited by R. J. H. Clark and R. E. Hester (Wiley, New York, 1988), Vol. 15.
[46]D. W. Chandler and R. L. Farrow, J. Chem. Phys. **85**, 810 (1986).
[47]R. L. Farrow and D. W. Chandler, J. Chem. Phys. **89**, 1994 (1988).
[48]J. J. Hinchen and R. H. Hobbs, J. Chem. Phys. **65**, 2732 (1976).
[49]R. A. Copeland and F. F. Crim, J. Chem. Phys. **78**, 5551 (1983).
[50]A. D. DePristo, J. J. BelBruno, J. Gelfand, and H. Rabitz, J. Chem. Phys. **74**, 5031 (1981).
[51]A. D. DePristo and H. Rabitz, J. Chem. Phys. **72**, 4685 (1980).
[52]R. A. Copeland and F. F. Crim, J. Chem. Phys. **81**, 5819 (1984).
[53]J. J. BelBruno, J. Gelfand, and H. Rabitz, J. Chem. Phys. **78**, 3990 (1983).
[54]L. Bonamy, J. Bonamy, D. Robert, B. Lavorel, R. Saint-Loup, R. Chaux, J. Santos, and H. Berger, J. Chem. Phys. **89**, 5568 (1988).
[55]C. G. Gray and H. L. Welsh, in *Essays in Structural Chemistry,* edited by A. J. Downs, D. A. Long, and L. A. K. Staveley (Plenum, New York, 1970), pp. 163–188.
[56]W. Meier, G. Ahlers, and H. Zacharias, J. Chem. Phys. **85**, 2599 (1986).
[57]J. Wolfrum, Discuss. Faraday Soc. **84**, 1 (1987).
[58]The subroutine STEPIT was used to do the nonlinear fitting and is available as Program No. 307, Quantum Chemistry Exchange Program, Indiana University, Bloomington, IN.
[59]G. Zarur and H. Rabitz, J. Chem. Phys. **60**, 2057 (1974).
[60]H. Rabitz and S.-H. Lam, J. Chem. Phys. **63**, 3532 (1975).